OXFORD

Evolution, divergence, and convergence in the mandibles of opossums (Didelphidae, Didelphimorphia)

Francisco das Chagas Silva-Neto[a], **Silvia E. Pavan**[b] **and Diego Astúa**[a,*]

[a]Laboratório de Mastozoologia, Departamento de Zoologia, Universidade Federal de Pernambuco. Av. Prof. Moraes Rego, s.n. Cidade Universitária. 50670-901 Recife, PE, Brazil
[b]Department of Biological Sciences, California State Polytechnic University, Humboldt, 1 Harpst Street, Arcata, CA 95521, USA

*Address correspondence to Diego Astúa. E-mail: diego.astua@ufpe.br
Handling editor: Zhi-Yun Jia

Abstract

Didelphid marsupials are considered a morphologically unspecialized group with a generalist diet that includes vertebrates, invertebrates, and plant matter. While cranium and scapula variation has already been examined within Didelphidae, variation in mandible shape, usually associated with diet or phylogeny in other mammalian groups, has not yet been properly assessed in the family. We evaluated the variation in mandible shape and size of didelphids (2470 specimens belonging to 94 species) using 2D geometric morphometrics. We classified the diet of the didelphids into four broad categories to assess whether morphospace ordination relates to dietary habits. We also provided the most comprehensive phylogeny for the family (123 out of the 126 living species) using 10 nuclear and mitochondrial genes. We then mapped mandible size and shape onto that phylogeny for 93 selected taxa and ancestral size and shapes were reconstructed by parsimony. We found phylogenetically structured variation in mandible morphology between didelphid groups, and our results indicate that they have a significant phylogenetic signal. The main axis of shape variation is poorly related to size, but the second is strongly allometric, indicating that allometry is not the main factor in shaping morphological diversity on their mandibles. Our results indicate that the shape and size of the ancestral mandible of didelphids would be similar to that of the current species of the genus *Marmosa*.

Key words: mandible, Didelphimorphia, morphological evolution, allometry, phylogeny, diet.

The order Didelphimorphia currently consists of a single family, Didelphidae, with 18 genera and 126 species (Astúa et al. 2022; Voss 2022; Miranda et al. 2023) with 90% of the species and 50% of the genera being endemic to South America (Voss and Jansa, 2009; Jansa et al. 2014). Didelphimorphia is the largest group of living marsupials in the Americas (Goin et al. 2016). They are classified into four subfamilies: Glironiinae (*Glironia*), Caluromyinae (*Caluromys* and *Caluromysiops*), Hyladelphinae (*Hyladelphys*), and Didelphinae (composed of four tribes, Marmosini, Metachirini, Didelphini, and Thylamyini, which include all remaining genera) (Voss and Jansa 2009). Despite having a conservative morphology and diet, didelphids show considerable variation in their body sizes and ecology (Astúa 2015; Amador and Giannini 2020; Voss and Jansa 2021). Adult specimens range from 10 g in the smallest species to 5 kg in *Didelphis virginiana* (Voss and Jansa 2021), and most species have generalist feeding habits, consuming a wide range of invertebrates, flowers, nectar, vertebrates, and fruits, in different proportions (Lessa et al. 2022). However, some species seem to have differences in food preferences: some *Caluromys* species have presented 75% of their diet composed of fruit remains (albeit the same species may switch to a predominantly insectivorous diet depending on food availability), *Chironectes* and *Lutreolina* species are usually considered to have predominantly carnivorous habits (although varied invertebrates and fruits are also recurrently

consumed), and most small-bodied species (Hyladelphinae, Marmosini, and Thylamyini) are usually seen as more insectivorous, yet do consume fruits and even some small vertebrates, depending on the taxon (Atramentowicz 1988; Astúa 2015; Voss and Jansa 2021; Lessa et al. 2022).

In mammals, mandible shape is usually related to diet and feeding behaviors, and has a primary function in capturing and processing food (Prevosti et al. 2012). The size and shape variation of the mandible has been studied in several mammalian groups, such as in primates (Meloro et al. 2015), rodents (Álvarez et al. 2011), ungulates (Raia et al. 2010), and carnivores (Christiansen, 2008). In turn, variation in cranial shape (Chemisquy et al. 2021) and scapula (Astúa 2009) in Didelphidae has already been analyzed, and recently Brum et al. (2022) have evaluated variation in size and shape in the mandibles in a subset of species from all three orders of American marsupials. Their analysis, however, used fewer species than ours and lacked some key taxa, thus hindering a complete understanding of shape diversification in Didelphidae, and they assumed discrete trophic categories in Didelphidae, which may be an oversimplification.

Didelphids, like all marsupials have functional needs in altricial newborns, which crawl into the mother's marsupium (when present) and attach to the nipple before suckling over a long period of lactation (Gemmell et al. 2002; Bennett and Goswami 2013). To fulfill this function, the skulls of newborn

marsupials are early ossified in the oral region (including the anterior portion of the mandible, premaxillae, maxillae, palatines, and pterygoids) for feeding (Clark and Smith 1993). These needs are considered constraints and are hypothesized to result in less morphological disparity and greater integration (less evolutionary flexibility) relative to placental mammals in terms of the oral apparatus (Goswami et al. 2012; Prevosti et al. 2012), and should thus also influence mandible shape.

However, didelphid marsupials exhibit unexpected and often underestimated morphological variations (Amador and Giannini 2016). Studies on the size and shape of structures such as the cranium, the scapula, or the molars indicate important variation among the main clades of Didelphidae (Astúa 2009; Chemisquy et al. 2015, 2021; Magnus and Cáceres 2017). Thus, didelphids constitute an interesting group to evaluate the effects of size, phylogenetic relatedness, and to some extent, diet, on mandible morphology. In this study, we evaluated the morphometric variation and differentiation (in size and shape) of the mandibles of living species of Didelphidae using the densest taxonomic sampling to date. We examined the role of phylogeny and diet in the shape and size of didelphid mandibles, and for that, we produced a dated phylogeny virtually complete for extant species (only three extant Didelphidae species not included), using nuclear and mitochondrial genetic data. Finally, we used these data to reconstruct the shape and size of the ancestral mandible of didelphids, to infer the evolution of the size and shape of this structure.

Materials and Methods

Taxon and gene sampling for the phylogenetic framework

In order to construct a dataset with several molecular markers and increased taxonomic density, that provides a reliable and virtually complete phylogenetic framework at the species level for extant didelphids, we used GenBank sequences available for ten genes, used by previous studies with the family Didelphidae (e.g., Voss and Jansa 2009; Jansa et al. 2014; Amador and Giannini 2016; Beck and Taglioretti 2019). Selected sequences included four mitochondrial genes: cytochrome *b* (*Cyt-b*), cytochrome *c* oxidase subunit 1 (*COI*), and the ribosomal subunits 12S and 16S; and six nuclear genes: interphotoreceptor retinoid-binding protein (IRBP), breast cancer susceptibility protein 1 (BRCA1), dentin matrix protein 1 (DMP1), recombination activating protein 1 (RAG1), von Willebrand factor (vWF), and transthyretin intron 1 (TTR). For each terminal species, we carefully selected DNA sequences from the same vouchers whenever possible. When combining sequences from different vouchers to compose a given terminal, we prioritized specimens belonging to the same haplogroups (as indicated by previous intraspecific phylogenetic analyses). A complete list of the sequences used with their respective GenBank accession codes, as well as the voucher information, is provided as Supporting information (Supplementary Table S1). We obtained DNA sequence data from 123 out of the 126 living Didelphidae species currently recognized (Voss 2022). The only three Didelphidae taxa not included are *Gracilinanus dryas*, *Monodelphis unistriata*, and *Philander deltae*, for which no sequence data is currently available in GenBank. We generally followed the classification on the

latest taxonomic compilation of Didelphidae (Voss 2022), although we considered four additional Didelphidae terminals in our analyses, representing four taxa listed as synonyms by Voss (2022): *Marmosa meridae*, *Marmosa limae*, *Thylamys citellus*, and *Thylamys pulchellus*. *Marmosa meridae* is considered a synonym of *M. demerarae* by Voss (2022), but phylogenetic analyses by Voss et al. (2020) recover specimens identified as *M. meridae* as sister to the Phaea species group (including *Marmosa constantiae*, *M. phaea*, and *M. demerarae*). Therefore, specimens currently identified as *M. meridae* are not sister nor nested within *M. demerarae*, and phylogenetically, they cannot be included within the same terminal as *M. demerarae*. To include this form that has been indicated as phylogenetically distinct from other recognized species, we keep a separate terminal identified as *M. meridae*. *M. limae* is also considered a synonym of *M. demerarae* (Voss 2022), based on the fact that specimens recognized as this putative species and associated with the name *limae* by Voss et al. (2020) do not seem to be phenotypically distinguishable from *M. demerarae*. Still, a genetically distinct haplogroup (associated with *M. limae*) is consistently recovered on phylogenetic analyses (Silva et al. 2019; Voss et al. 2020), and to retain as much as possible of the phylogenetic diversity within Didelphidae represented in our phylogeny (which can also be used by future comparative analyses), we kept a terminal representing *M. limae*. *Thylamys citellus* and *T. pulchellus* are considered synonyms of *T. pusillus* (Giarla et al. 2010; Voss 2022), but we recognized separate terminals for those taxa following taxonomic conclusions of Teta et al. (2009), an arrangement also followed by recent taxonomic compilations (Teta et al. 2018; Astúa et al. 2022). By recognizing four distinct terminals for those taxonomically debated taxa, we mean to provide a complete phylogenetic framework, and the opportunity to include those putative species in our and future comparative analyses. We followed Amador and Giannini (2016) for outgroup taxa and included *Rhyncholestes raphanurus*, *Lestoros inca*, *Caenolestes fuliginosus*, *Dromiciops gliroides*, and *Dasyurus geoffroii*. Thereby, the analysis comprised a total of 132 terminals (127 Didelphidae terminals and five outgroup terminals).

Sequence alignment, phylogenetic, and time-calibration analyses

DNA sequences from each gene selected were aligned using MUSCLE version 3.8.425 (Edgar 2004) as implemented by Geneious Prime version 2022.2.1 (https://www.geneious.com) using default parameters. We then concatenated sequence data from all genes into a combined-gene dataset in Geneious and used PartitionFinder2 version 2.1.1 (Lanfear et al. 2017) to select the best partitions and models of nucleotide substitution under the Bayesian information criterion (Schwarz 1978). We defined separate data blocks for the three codon positions for all ten genes used and set PartitionFinder2 to search for every nucleotide model available.

We performed phylogenetic analyses using maximum likelihood (ML) in Garli 2.10 (Zwickl 2006) using default parameters on the Cipres Portal (Miller et al. 2010). The best-fit partitioning schemes and models for each dataset were specified as determined by PartitionFinder2, and the model parameters were set to be estimated from the data. A total of

two independent searches were performed, and nodal support was assessed by 1000 bootstrap pseudoreplicates. Bootstrap values were summarized in SumTrees version 4.0.0 using DendroPy 4.0.3 (Sukumaran and Holder 2010).

We used the ML implementation of RelTime (Tamura et al. 2018) in MEGA 11 (Tamura et al. 2021) to perform time calibration on the phylogeny. For this analysis, we used the ML tree generated in Garli and our concatenated dataset. We followed Jansa et al. (2014) to set calibration points. We used two minimum divergence dates based on fossil data, and assumed a lognormal distribution with a standard deviation of 1 for each, with the following offsets: (1) the divergence between *Didelphis* and *Philander* at 3.3 Ma; (2) the split between *Monodelphis* and *Marmosa* at 12.1 Ma. Additionally, we calibrated the most recent common ancestor of Didelphidae by implementing a normally distributed prior with mean = 26.3 Ma and standard deviation = 3.2 Ma, following the estimates of Jansa et al. (2014) for the crown age of Didelphidae. The evolutive model used was the GTR + I + G, selected as the best model for the entire (unpartitioned) dataset.

Sample for morphometric analyses

We examined a total of 2,470 specimens, from 17 genera and 94 extant species of Didelphidae (representing 94% and 75% of extant genera and species, respectively). These specimens are housed in the mammal collections of the following institutions: American Museum of Natural History (AMNH), Bell Museum of Natural History, University of Minnesota (MMNH), Carnegie Museum (CM), Coleção de Mamíferos, Departamento de Zoologia da Universidade Federal de Minas Gerais (UFMG), Coleção de Mamíferos, Universidade Federal da Paraíba (UFPB), Coleção de Mamíferos, Universidade Federal de Pernambuco (UFPE), Coleção de Mamíferos, Universidade Federal de Santa Catarina (UFSC), Colección de Mamíferos Lillo (CML), Colección Nacional Patagonica (CNP), Field Museum of Natural History (FMNH), Michigan State University Museum (MSU), Museo de Historia Natural de la Universidad Nacional Mayor de San Marcos (MUSM), Museu de Ciências Naturais da Pontifícia Universidade Católica de Minas Gerais (MCN), Museu de Ciências Naturais da Ulbra (MCNU), Museu de História Natural Capão da Imbuia (MHNCI), Museu Nacional, Rio de Janeiro (MN), Museu Paraense Emílio Goeldi (MPEG), Museu de Zoologia da Universidade de São Paulo (MZUSP), Museum of Natural Science, Louisiana State University (LSUMZ), Museum of Southwestern Biology (MSB), Museum of Texas Tech University (TTU), Museum of Vertebrate Zoology (MVZ), National Museum of Natural History (USNM), Natural History Museum, University of Kansas (KU), Royal Ontario Museum (ROM), Sam Noble Oklahoma Museum of Natural History (OMNH), and University of Wisconsin Zoological Museum (UWZM). A complete listing of species included in this study, with their respective sample sizes, is presented in Table 1.

We used only adult specimens with fully erupted dentition to avoid the influence of ontogenetic variation (Tyndale-Biscoe and Mackenzie 1976; Tribe 1990; Astúa and Leiner 2008). Whenever possible, we sampled an equal number of males and females, up to 30 per species, to capture intra-specific variance. For rarer taxa, all available specimens were included in the analysis. As we are interested in family-wide variation and diversification, and given the low sample sizes for rarer species, we pooled sexes in all analyses.

Images and landmarks

All the images used in the analysis included a ruler for scale. The mandibles were positioned aligning the coronoid process parallel to the camera base and lens, with the lateral view of the mandible exposed to be photographed. Most pictures were taken from the right dentary. When the right dentary was damaged to the point of preventing the placement of the landmarks, the left dentary was used, digitally inverted to match the alignment used for the other specimens. In each image, we digitized 16 landmarks and 8 semi-landmarks to capture the mandible shape, as shown in Figure 1 and defined in Table 2. Landmarks were set using the software tpsDig2, version 2.31 (Rohlf 2015).

All landmark coordinates were tested for repeatability. Thirty specimens from one species were randomly chosen and all landmarks were digitized twice, on different days, in a different sequence, by the same observer. We estimated repeatability as the intraclass correlation coefficient, derived from an analysis of variance on the x and y coordinates of each landmark, using the specimens as a factor (Falconer and Mackay 2009). All coordinates presented repeatabilities between 0.98 and 0.99 and were considered satisfactory for subsequent analyses.

Size and shape variation

Sliding of the semi-landmarks during a generalized procrustes analysis (GPA) was previously conducted in tpsRelw, version 1.75 (Rohlf 2015). The semi-landmarks were allowed to slide along their tangent directions to minimize the Procrustes distance between specimens (Bookstein 1997). After superimposition and sliding, coordinates were scaled back to their original centroid sizes resulting in Boas coordinates (Bookstein 2018, 2021), and the aligned semi-landmarks were then treated as landmarks in subsequent analyses. We exported the Boas coordinates into MorphoJ, version 1.07a (Klingenberg 2011).

We then aligned landmark configurations by performing a new GPA, thus removing all information related to the position, orientation, and isometric size of the mandibles (Rohlf and Slice 1990). Shape variation and the distribution of specimens in morphospace were assessed by a principal component analysis (PCA) of the Procrustes coordinates, where the resulting principal components (PCs) correspond to the main axes of shape variation in the samples studied.

Aligned landmark coordinates were used to perform a multivariate regression between size and shape, using Procrustes coordinates as the dependent variables, and log (centroid size) as the independent variable, to assess the overall effect of size on shape (allometry) in the whole sample (Klingenberg 2016). The significance of this relationship was analyzed by performing a permutation test with 10,000 replicates. Because species have different sample sizes, more numerous samples could artificially alter the regression results. Thus, we used the average for each species (i.e., one point per species) in the allometry test, and allometry was evaluated through a phylogenetic generalized least squares (PGLS) to account for the phylogenetic relationships between taxa (Martins and Hansen 1997; Adams 2014). For this, we used the phylogenetic hypothesis obtained in the previous step. We pruned the

Table 1 Specimens analyzed and respective sample sizes. Asterisks indicate species not used in ancestral size and shape reconstructions

Genus/species	*n*	Genus/species	*n*
Caluromys		*Marmosops* (cont.)	
Caluromys derbianus	68	*Marmosops carri*	38
Caluromys lanatus	61	*Marmosops caucae*	3
Caluromys philander	104	*Marmosops chucha*	3
Caluromysiops		*Marmosops fuscatus*	1
Caluromysiops irrupta	5	*Marmosops incanus*	64
Chironectes		*Marmosops invictus*	8
Chironectes minimus	54	*Marmosops noctivagus*	75
Cryptonanus		*Marmosops ocellatus*	18
Cryptonanus agricolai	10	*Marmosops parvidens*	11
Cryptonanus chacoensis	7	*Marmosops paulensis*	32
Cryptonanus guahybae	17	*Marmosops pinheiroi*	19
Cryptonanus unduaviensis	6	*Metachirus*	
Didelphis		*Metachirus aritanai*	1
Didelphis albiventris	60	*Metachirus myosurus*	56
Didelphis aurita	57	*Monodelphis*	
Didelphis imperfecta	16	*Monodelphis adusta*	19
Didelphis marsupialis	65	*Monodelphis americana*	51
Didelphis pernigra	66	*Monodelphis arlindoi*	22
Didelphis virginiana	19	*Monodelphis brevicaudata*	40
Glironia		*Monodelphis dimidiata*	23
Glironia venusta	4	*Monodelphis domestica*	73
Gracilinanus		*Monodelphis emiliae*	12
Gracilinanus aceramarcae	7	*Monodelphis gardneri*	1
Gracilinanus agilis	67	*Monodelphis glirina*	74
*Gracilinanus dryas**	8	*Monodelphis handleyi*	3
Gracilinanus marica	9	*Monodelphis iheringi*	16
Gracilinanus microtarsus	33	*Monodelphis kunsi*	2
Hyladelphys		*Monodelphis osgoodi*	1
Hyladelphys kalinowskii	3	*Monodelphis palliolata*	8
Lestodelphys		*Monodelphis peruviana*	6
Lestodelphys halli	12	*Monodelphis pinocchio*	2
Lutreolina		*Monodelphis reigi*	1
Lutreolina crassicaudata	53	*Monodelphis saci*	13
Lutreolina massoia	1	*Monodelphis sanctaerosae*	1
Marmosa		*Monodelphis scalops*	8
Marmosa adleri	4	*Monodelphis touan*	24
Marmosa alstoni	11	*Monodelphis vossi*	3
Marmosa constantiae	12	*Philander*	
Marmosa demerarae	53	*Philander andersoni*	39
Marmosa germana	4	*Philander mcilhennyi*	15
Marmosa isthmica	57	*Philander melanurus*	59
Marmosa jansae	2	*Philander opossum*	49
Marmosa lepida	6	*Philander quica*	62
Marmosa mexicana	47	*Thylamys*	
Marmosa murina	57	*Thylamys elegans*	46
Marmosa paraguayana	48	*Thylamys karimii*	16
Marmosa parda	4	*Thylamys macrurus*	4
Marmosa phaea	11	*Thylamys pallidior*	74
Marmosa rapposa	11	*Thylamys pusillus*	10
Marmosa rubra	17	*Thylamys sponsorius*	21
Marmosa rutteri	48	*Thylamys tatei*	10
Marmosa tyleriana	8	*Thylamys venustus*	10

Table 1. Continued

Genus/species	n	Genus/species	n
Marmosa xerophila	60	***Tlacuatzin***	
Marmosops		*Tlacuatzin balsasensis*	5
Marmosops bishopi	4	*Tlacuatzin sinaloae*	42
Total			2470
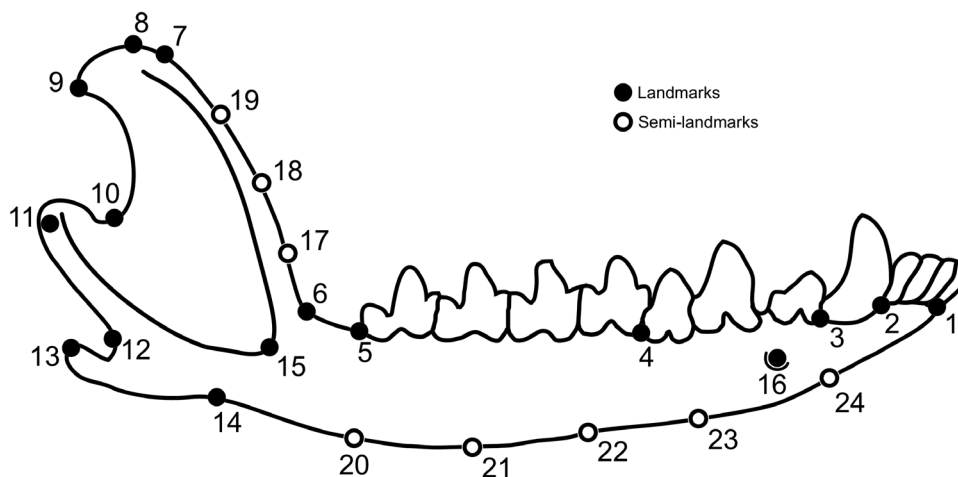
Figure 1 Landmarks and semi-landmarks used in these analyses, shown on a mandible of *Tlacuatzin* (based on specimen KU 89200). Landmark and semi-landmark definitions and locations are presented in Table 2.

Table 2 Landmarks and semi-landmarks used in this study

Number	Position
1	Anterior base of first lower incisor
2	Posterior base of fourth lower incisor
3	Posterior base of lower canine
4	Posterior base of third lower premolar
5	Posterior base of fourth lower molar
6	Inflexion point between the horizontal ramus of the mandible and the coronoid process (anterior base of the coronoid process)
7	Inflexion point at the top of the coronoid process anterior border
8	Superior tip of the coronoid process
9	Superior tip of the posterior border of the coronoid process
10	Inflexion point at the base of the posterior border and the coronoid process toward the articular process
11	Labial tip of the articular process
12	Posterior base of the angular process
13	Tip of the angular process
14	Anterior base of the angular process
15	Antero-ventral tip of the masseteric fossa border
16	Anterior mentonian foramen
17–19	Equally distant semi-landmarks along the anterior border of the coronoid process
20–24	Equally distant semi-landmarks along the ventral border of the horizontal ramus

major topology, removing all taxa for which we did not have morphological samples, and excluded from the morphometric sample *G. dryas*, as it is absent from our phylogeny. GPA and PCA analyses were performed using MorphoJ, version 1.07a (Klingenberg 2011), and PGLS was performed using the *procD.pgls* function (λ = 1; iter = 999) of the *geomorph* (Baken et al. 2021; Adams et al. 2022) package for R (R Core Team 2021). Changes along the PCs are shown as warped outlines, based on the outline of the specimen pictures in Figure 1, as described in the documentation of MorphoJ and in Klingenberg (2013). We also performed linear correlation tests between centroid size and coordinates of the first five

PCs using the software PAST, version 4.02 (Hammer et al. 2001), to assess the relative importance of size on the major axes of shape variation.

Phylogeny and morphological variation

We assessed the relation between morphology and phylogeny by constructing a phylomorphospace, mapping a phylogeny onto the morphospace (Sidlauskas 2008), using the pruned phylogenetic hypothesis we obtained in the previous step. Therefore, we used 93 species average Procrustes coordinates for the construction of the phylomorphospace. We tested our morphometric data for a phylogenetic signal in size and shape using a permutation test. Significance was tested by 999 random permutations of the shape data between the nodes of the phylogeny. A strong phylogenetic signal exists if more related taxa are phenotypically more similar than taxa that are phylogenetically more distant (Klingenberg and Gidaszewski 2010). These analyses were performed in MorphoJ for size (Klingenberg 2011) and the function *physignal* in *geomorph* for shape (Baken et al. 2021) package for R (R Core Team 2021).

Diet

To visually estimate any effect of diet on mandible shape variation, we defined coarse groupings based on recent compilations on the diet of Neotropical marsupials and the original literature cited therein (Santori et al. 2012; Astúa, 2015; Voss and Jansa 2021; Lessa et al. 2022). Opossums' diets consist of vertebrates, invertebrates, and fruits/plant matter, with distinct species varying mostly in the relative

Table 3 Broad diet classes used and genera assigned to each class. See text for further details

| Diet class	Genera
Omnivores	*Didelphis*, *Philander*
Omnivores with fruit preference	*Caluromys*, *Caluromysiops*
Omnivores with invertebrate preference	*Glironia*, *Gracilinanus*, *Hyladelphys*, *Lestodelphys*, *Marmosa*, *Marmosops*, *Metachirus*, *Monodelphis*, *Thylamys*, *Tlacuatzin*
Omnivores with vertebrate preference	*Chironectes*, *Lutreolina*

proportions of these items. Comprehensive diet studies provide no evidence that any opossum species feeds on only one of these categories. While some previous studies (e.g., Chemisquy et al. 2015, 2021; Brum et al. 2022) have used feeding categories, it should be clear that separating taxa into discrete diet categories is subjective, as diet in opossums represents mostly a continuum (Astúa de Moraes et al. 2003). The most frequently used category system for opossum diets is derived from Figure 1 in Vieira and Astúa de Moraes (2003), which was designed only as an illustration of such a continuum and not to be used as discrete categories (as stated explicitly in a new version of that illustration in Lessa et al. 2022). However, as diet is often related to morphology in mammals, and as no quantitative nor objective assessment exists for diet classification or quantification in opossums, we roughly classified opossum diet preferences into four main types: omnivores, omnivores with a preference for fruits, omnivores with a preference for invertebrates, omnivores with a preference for vertebrates (Table 3). These categories somewhat overlap with more traditional denominations (omnivores, frugivores, insectivores, and carnivores) used in other studies, but we avoided using those terms as they can be misleading as they have embedded the notion that the diets are distinct. While ours are also formally discrete categories (each taxon is assigned to a single group) we hope they convey that they are all actual slight variations of an overall omnivore diet. As most species lack adequate diet data (Astúa 2015), we used data from phylogenetically related species to assign species to a given feeding category and assigned all species in a single genus to the same group (i.e., if only a few species from a genus had some information available on diet, we extrapolated that information to all members of the genus). To assess whether the ordination resulting from the PCA could be related to feeding habits, taxa were classified by diet in PCA on MorphoJ, version 1.07a (Klingenberg 2011). We avoided using other discriminant or canonical variates analyses because of the existing uncertainty in these diet estimates, and thus on the resulting a priori groupings.

Ancestral size and shape reconstruction

We reconstructed the hypothetical sizes and shapes at different nodes along the phylogeny for the opossum mandible,

Table 4 Character sampling, number of sequences (=terminals) for each gene, number of aligned base pairs (bp), and best-fitting models of nucleotide substitution. See Methods for gene abbreviations

Gene	Included sequences	Aligned bp	Selected model/partitions
Cyt-b	129	1149	GTR + I + G for 1st position, HKY + I + G for 2nd, GTR + I + G for 3rd
COI	42	642	TRNEF + I + G for 1st position, F81 for 2nd, HKY + G for 3rd
12S	36	874	GTR + I + G for 1st, 2nd, and 3rd positions
16S	27	2163	GTR + I + G for 1st, 2nd, and 3rd positions
IRBP	91	1158	GTR + I + G for 1st position, TVM + I + G for 2nd, TIMEF + G for 3rd
BRCA1	109	2103	GTR + G for 1st position, K81UF + G for 2nd, HKY + G for 3rd
DMP1	41	1206	GTR + G for 1st position, GTR + G for 2nd, TIMEF + G for 3rd
RAG1	41	2790	GTR + I + G for 1st position, TVM + I + G for 2nd, GTR + G for 3rd
vWF	41	957	GTR + I + G for 1st position, TVM + I + G for 2nd, TIMEF + G for 3rd
TTR	27	1764	HKY + G for 1st, 2nd, and 3rd positions
Total	584	14,806	
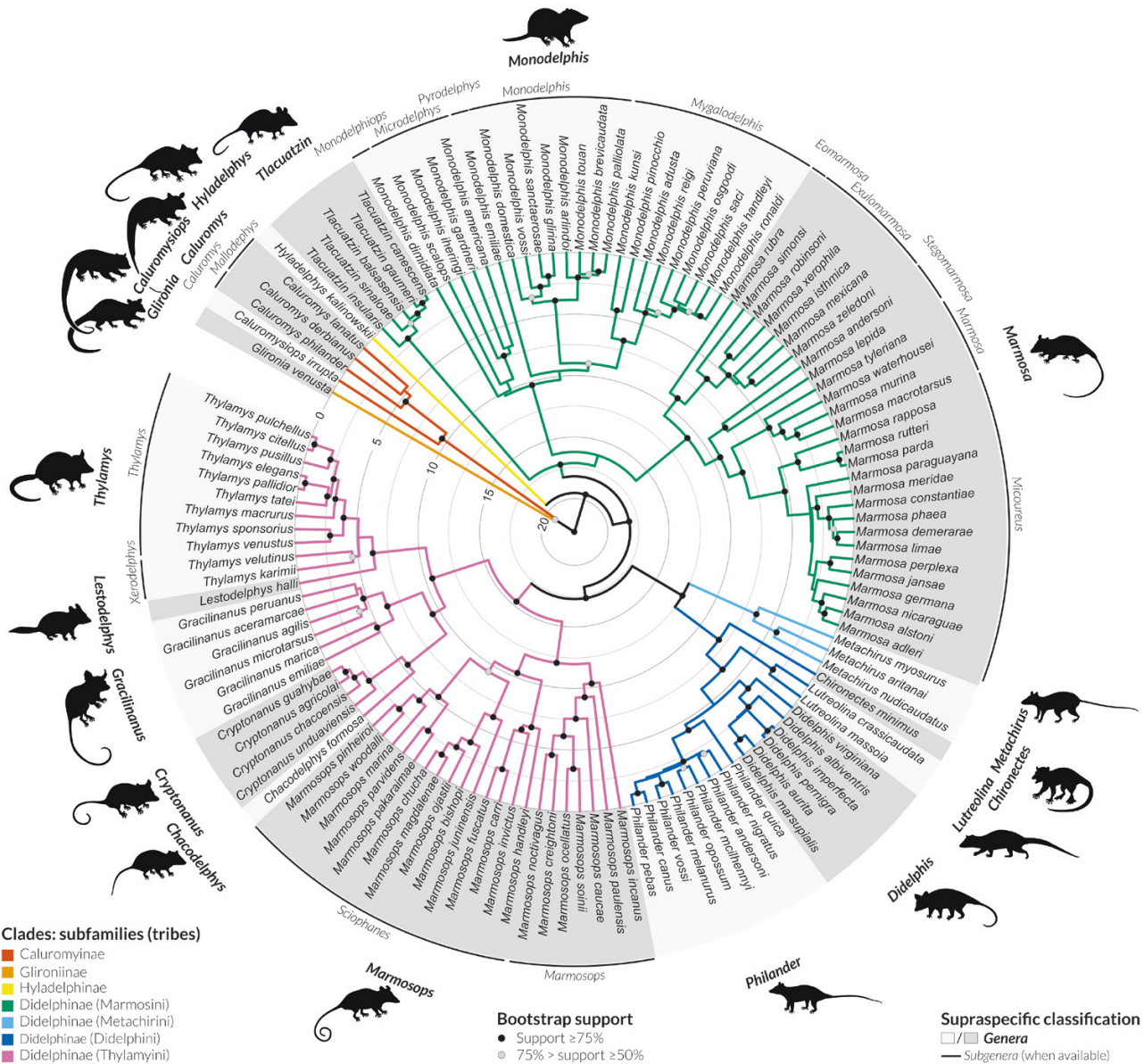
Figure 2 Time-calibrated maximum-likelihood phylogeny for Didelphidae based on analyses of the combined-gene dataset for 126 ingroup terminals and 5 outgroup taxa (not shown). Subfamilies and tribes within Didelphinae are indicated by color codes along the branches, and bootstrap values are indicated (only nodes with bootstrap values above 50% are indicated). For genera with existing subgeneric classification, subgenera are indicated above terminals. Illustration generated using iTOL v5 (Letunic and Bork 2021), genera silhouettes by M. Cavalcanti and P. Pilatti.

using the same pruned tree and morphological dataset used for creating the phylomorphospace. For hypothetical sizes, we used the average centroid sizes for each species. For shapes, we used the mean shape for each species (calculated as the mean of aligned coordinates). Ancestral sizes and shapes were reconstructed using squared-change parsimony, in Mesquite, version 3.70 (Maddison and Maddison 2021) and TpsTree, version 1.24 (Rohlf 2015). Living species were used as references for the interpretation of the inferred ancestral morphologies. For size estimates of some selected nodes, the closest-sized species were used as a reference. For shape, all shapes (average shapes for all current species and shapes from all reconstructed nodes) were included in a single matrix, and all pairwise distances were calculated with TpsSmall software, version 1.36 (Rohlf 2015). We then used the closest living species in shape to compare with selected nodes.

Results

Phylogeny and divergence times

Characteristics of our combined-gene dataset, together with best-fitting models of sequence evolution for each partition are summarized in Table 4. The final alignment included a total of 14.806 characters, with 28.8% of missing data. The tree recovered includes 97.6% of extant Didelphidae diversity (123 out of the 126 currently recognized species), and is shown in Figure 2 with accompanying nodal support values. A complete list of the sequences used in this analysis, along with the respective voucher numbers, is provided as Supplementary data (Table S1).

The family Didelphidae was recovered as monophyletic with high nodal support, as well as all currently recognized subfamilies and genera. In fact, only two intergeneric clades are not strongly supported (with bootstrap values between

50% and 75%): (1) the sister relationship between the genus *Glironia* and the subfamily Caluromyinae, and (2) the sister relationship between the genus *Marmosa* and *Monodelphis*. Subgenera and species groups, as listed by Voss (2022), were also recovered as monophyletic in our analysis, most of which with high nodal support. Exceptions (either weakly or moderately supported groups) include the subgenera *Mallodelphys*, *Microdelphys*, *Sciophanes*, and *Xerodelphis*.

Divergence time estimates based on RelTime analysis (Figure 2) suggest the first diversification of Didelphidae close to the Oligocene-Miocene boundary (median age 22.71 Ma), and subsequent diversification events between Didelphidae subfamilies in the early Miocene (median ages between 20.85 and 19.54 Ma). Diversification events within genera spanned a broad period of time, with some genera starting to diversify as early as the middle–late Miocene (e.g., median ages 11.98, 10.77, and 10.30 Ma for *Marmosops, Marmosa, and Monodelphis*, respectively), while others did not start to diversify until the late Pliocene–early Pleistocene (e.g., median ages 1.97, 2.06, and 2.09 Ma for *Tlacuatzin, Philander, and Cryptonanus*, respectively). Files with the final topology with branch lengths, including bootstrap values, and with the time-calibrated phylogeny are provided as Supplementary data.

Size and shape variation

The result of PCA on the shape variables is presented in Figure 3. The first principal component (PC1) explains 42.04% of the total variation in shape and is associated with a horizontal ramus becoming more slender, an elongation of the angular process, a shortening of the coronoid process, and a decrease of the angle between the coronoid process and the horizontal ramus. Negative scores are associated with specimens with relatively shorter mandibles, robust (wide) horizontal rami, relatively shorter and inconspicuous angular processes, and longer and more posteriorly oriented coronoid processes (represented mainly by *Caluromys*). Positive scores are associated with narrower horizontal rami, delicate and well-defined angular processes, and coronoid processes that are shorter and more vertically oriented. We observe an overlap between all other species toward the positive scores. Thus, the main axis of shape variation is driven by the difference between the unique shape of the mandible of *Caluromys* and that of all other taxa. It shows only a weak correlation with size ($r = -0.17$, $P < 0.001$) as specimens with negative scores are intermediate in size, while specimens with positive scores include both the larger and the smaller taxa.

The second principal component (PC2) explains 24.08% of the total variation in shape and is associated with more robust mandibles, relatively wider coronoid processes with relatively larger masseteric fossae, and more dorsally inflected horizontal rami. This shape is represented mostly by *Didelphis*, *Lutreolina,* and *Philander* specimens, with an overlap with *Caluromysiops*. Specimens with negative scores have more slender horizontal rami and coronoid processes and straighter horizontal rami. On these scores, there is an overlap between Marmosini and Thylamyini, but also *Glironia* and *Hyladelphys*. *Caluromys* specimens are located in an intermediate position on PC2. PC2 is strongly ($r = 0.87$, $P < 0.001$) correlated with size, thus describing a strongly allometric shape variation. PCs 3–5 summarize 6.05%, 4.97%, and 4.14% of the total variation, respectively, and correlate poorly or not with size, with $r = 0.08$, $P < 0.001$, and $r = 0.19$, $P < 0.001$ (for PC3 and PC4, respectively), and no significant correlation for PC5. No clear ordination pattern
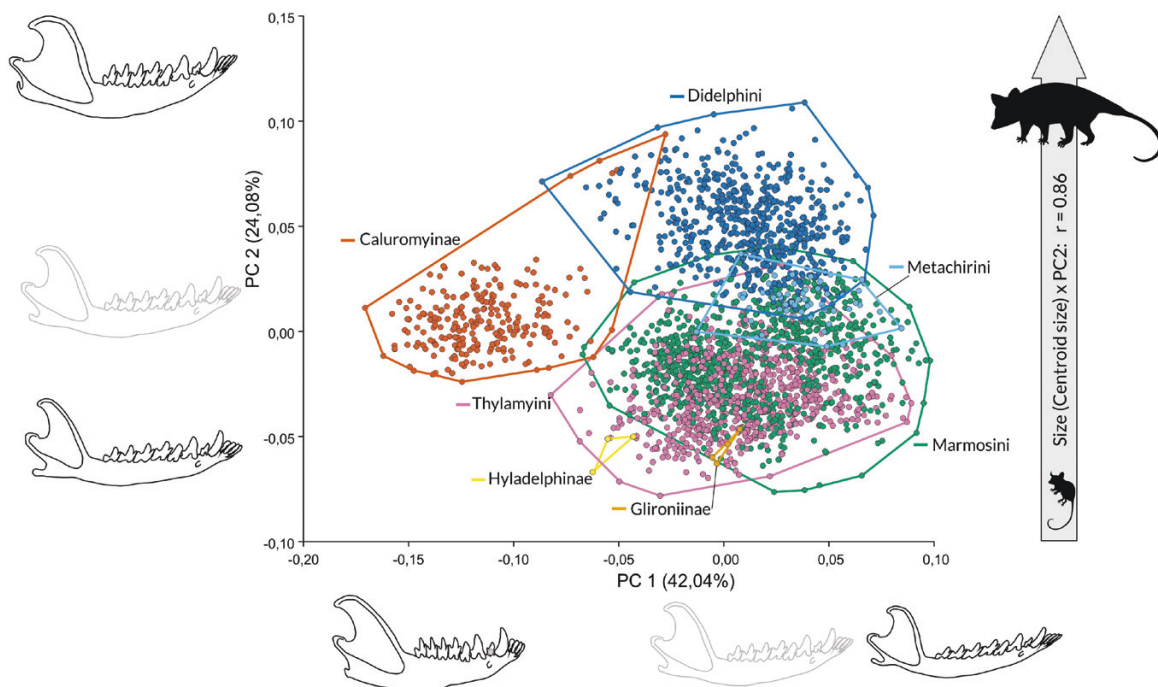
Figure 3 Principal components analysis on shape variables of the mandibles of Didelphidae. The two first components shown represent 66.12% of overall shape variation. Mandible outlines shown along PC1 and PC2 represent shape variations toward each axis end (black outline) as compared to the reference (grey outline). Mandible outlines are warped based on the deformation grids from the reference to the lowest and highest scores along each PC. Convex hulls indicate subfamilies or tribes within Didelphinae (color-coded as in Figure 2). The correlation of PC2 with centroid size is also indicated (see text for correlations of centroid size and other PCs).
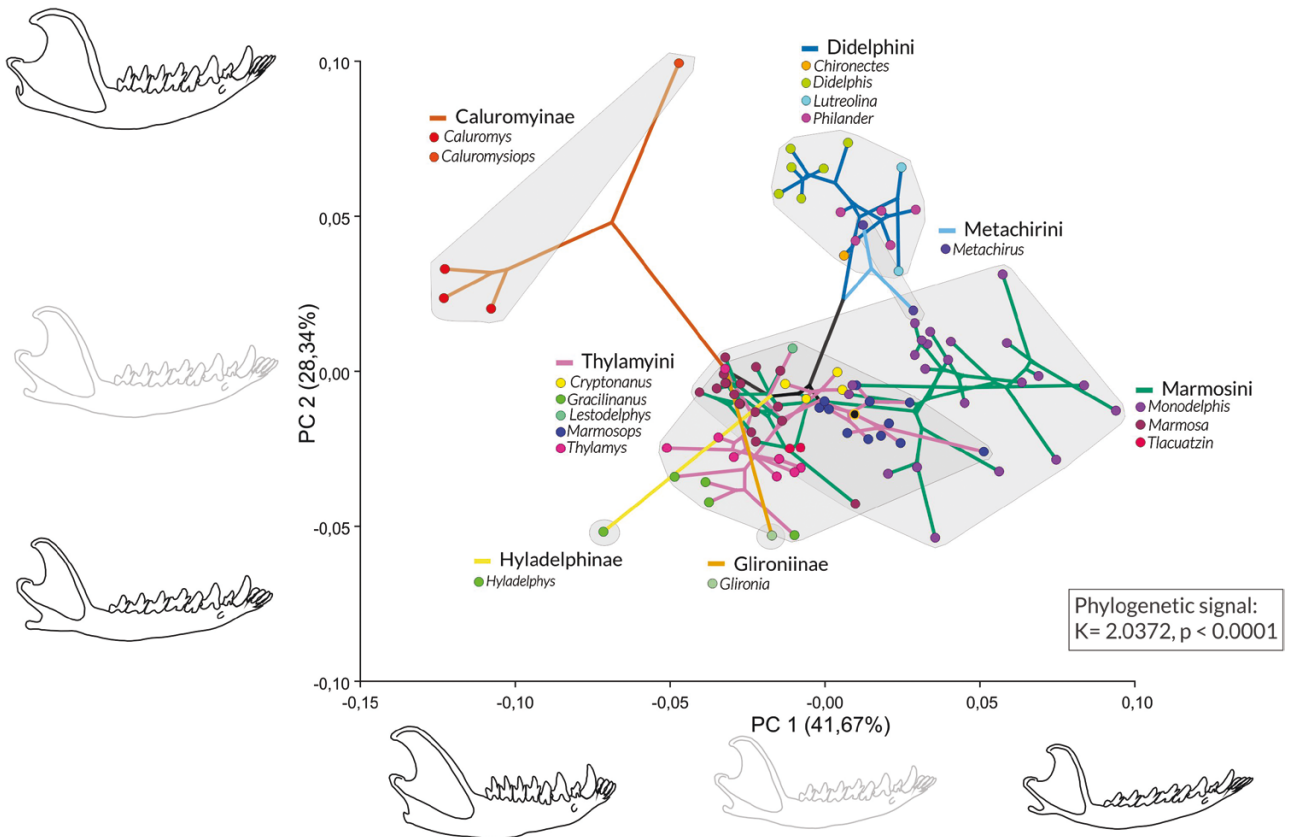
Figure 4 Phylomorphospace of mandibles, obtained by plotting the phylogeny from Figure 2, after pruning species absent from our dataset onto the morphospace defined by species means, and estimating scores for all internal nodes. Outlines shown along PC1 and PC2 represent shape variations toward each axis end (black outline) as compared to the reference (grey outline). Mandible outlines are warped based on the deformation grids from the reference to the lowest and highest scores along each PC. Gray areas indicate subfamilies or tribes within Didelphinae. Branches are labeled using the same coding as in Figure 2.

emerges from the inspection of PC3 onwards, they are not shown (PC1 × PC3 is provided as Supplementary Figure S1). The PGLS regression of shape as a function of size taking phylogeny into account revealed a significant but weak association between both variables ($F = 8.8$, $R^2 = 0.09$, $P < 0.001$).

There is a significant phylogenetic signal in shape variation ($K = 2.0372$, $P < 0.0001$), and the phylomorphospace shows an overall phylogenetic structure (Figure 4). The first two components concentrate around 70% of the shape variation across species means, and the overall position of species in the phylomorphospace repeats that of group centroids in the PCA with all specimens, with the shape difference of *Caluromys* mandible vs. all remaining taxa driving PC1 (Figures 3 and 4). The Caluromyinae are the most separated clade along a combination of PC1 and PC2, followed by the Didelphini, and with a partial overlap in morphospace between Thylamyini and Marmosini. However, divergences within clades reveal interesting patterns of divergence or convergence. Within Caluromyinae, *Caluromysiops* is highly divergent from *Caluromys* species, with a more robust mandible, in a unique position in morphospace. Metachirini, although more closely related to Didelphini, occupies an intermediate position between Didelphini and Marmosini morphospaces, with one species located in each of these morphospaces. *Glironia*, while more closely related to the Caluromyinae (with intermediate support) in our phylogeny, is highly divergent from the Caluromyinae taxa and occupies a position within the Thylamyini morphospace. Finally, *Hyladelphys* is highly

divergent from all other small opossums and also occupies a unique position in morphospace, outside that of Marmosini or Thylamyini. The three richest genera (*Monodelphis*, *Marmosa*, and *Marmosops*) have different patterns of morphospace occupation: *Monodelphis* species vary much more in shape (thus occupy a larger portion of the morphospace), while *Marmosa* and *Marmosops* occupy more restricted portions of morphospace (Figure 4). There is also a significant phylogenetic signal in size variation ($P < 0.001$) and plotting centroid size variation along with the phylogeny clearly shows the overlap of Marmosini, Thylamyini, Hyladelphinae, and Glironiinae, all sharing small mandibles, the overlap of Caluromyinae, Metachirini and *Lutreolina massoia* in an intermediate position, and all remaining Didelphine with larger mandibles, into two increase events (Supplementary Figure S3).

Diet

The result of the PCA on shape labeled according to the previously defined categories (Table 3) is shown in Figure 5. Three major groupings can be identified, albeit with partial overlaps. Omnivores with fruit preferences (*Caluromys* and *Caluromysiops*) overlap partially with omnivores: *Caluromys* specimens are the most apart from the other groups, occupying most of the negative scores of PC1, while *Caluromysiops* specimens overlap with omnivores (*Didelphis* and *Philander*) and are separated from *Caluromys* specimens, along PC2 (*Caluromysiops* centroid is the one labeled in green with
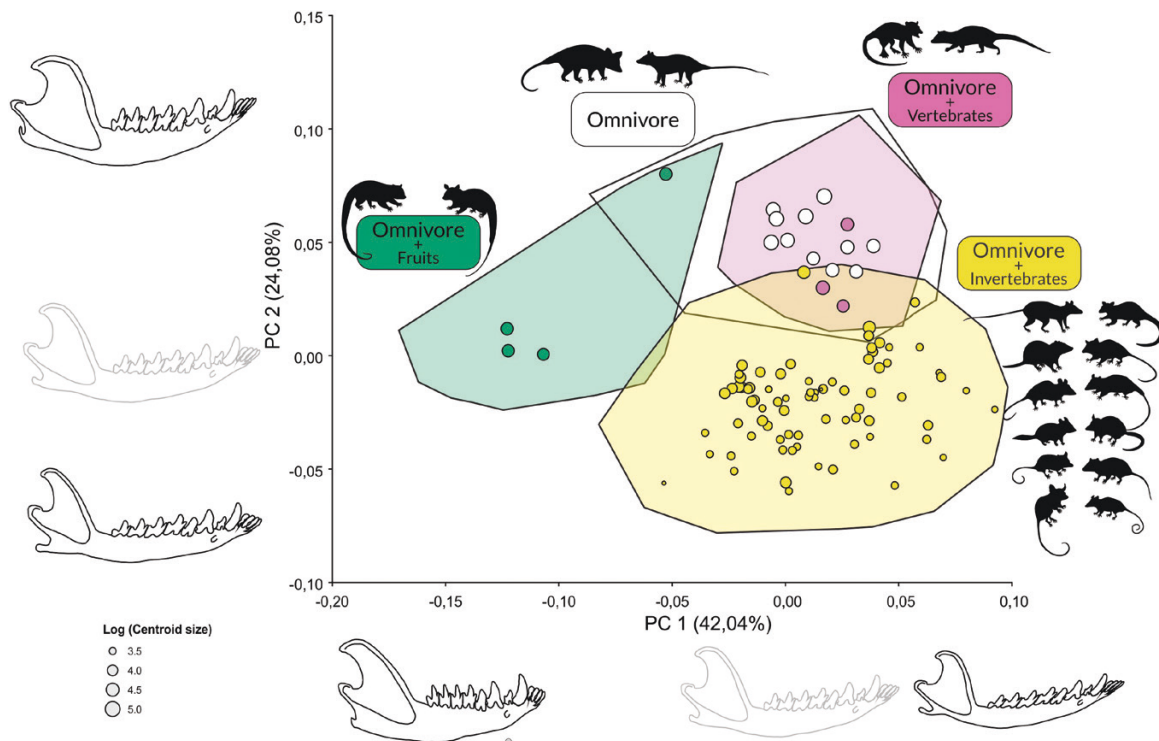
Figure 5 Principal components analysis on shape variables of the mandibles of Didelphidae, with taxa labeled by diet group, as defined in Table 3 and explained in the text. Hulls indicate morphospace occupation by all specimens in each diet group, and points represent species means within each group. Point sizes are scaled to log (centroid size). Outlines shown along PC1 and PC2 represent shape variations toward each axis end (black outline) as compared to the reference (grey outline). Mandible outlines are warped based on the deformation grids from the reference to the lowest and highest scores along each PC. Silhouettes represent genera (as presented in Figure 2) in each diet group (not to scale).

the highest PC2 scores). Omnivores with vertebrate preferences (*Lutreolina* and *Chironectes*) overlap completely with omnivores. All other taxa (omnivores with invertebrate preferences) are the best-defined group in the PCA, and overlap occurs only slightly with omnivores and species with vertebrate preferences.

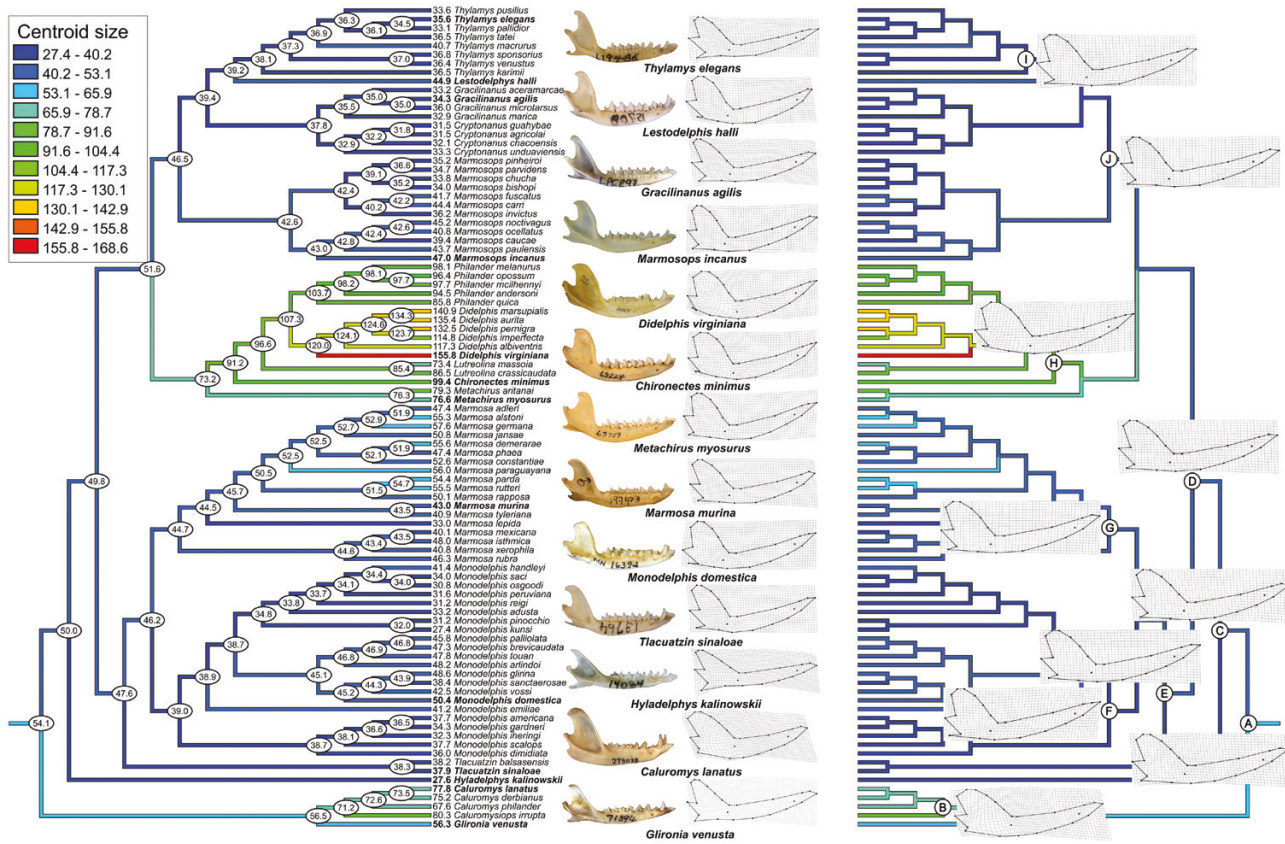## Ancestral size and shape reconstruction

The reconstructions of hypothetical ancestral mandible shapes and sizes of Didelphidae along the phylogeny are summarized in Figure 6 (see also Supplementary Figure S3 for an alternative visualization). The reconstructed mandible at the root of the Didelphidae phylogeny had a centroid size of 54.1 mm, which corresponds approximately to the sizes of the mandibles in *Marmosa parda* and *M. alstoni*. Along the phylogeny, we observe several events of size reduction, in Hyladelphinae, Marmosini, and Thylamyini, and two main events of size increase, in the Caluromyinae and the Didelphini + Metachirini clade. The two increasing events mentioned are of higher magnitude than any reduction observed. In both, size increases 31–35% from the overall Didelphidae ancestor to the ancestor of Caluromyinae or that of Didelphini + Metachirni. Size increases up to 48% in the largest Caluromyinae (*Caluromys lanatus*) and up to 187% in the largest Didelphini (*D. virginiana*). In contrast, size decreases from –12% to –14% from the Didelphidae ancestor to the ancestor of Thylamyini or Marmosini, and the decrease reaches –42% in the smallest Thylamyini (*Cryptonanus agricolai*), –50% in the smallest Marmosini (*Monodelphis kunsi*), and –49% in *Hyladelphys kalinowskii*, but extreme reductions are rare and the vast majority of

Thylamyini and Marmosini are more similar in size to the overall ancestor.

The reconstructed ancestral mandible shape for Didelphidae (node A in Figure 6) is very similar to most living species of the genus *Marmosa* (mainly) and, to a slightly lesser extent, *Thylamys*. Reconstructed mandible shapes on most of the other nodes remain similar to the ancestral condition, except for nodes B, referring to Caluromyinae, and H, referring to Didelphini (Figure 6). On these, we observe an increase in robustness mainly on the coronoid process and the horizontal ramus, along with the onset of deflection of the angular process typical of Caluromyinae.

Discussion

We present here the most complete dated phylogeny for the Didelphidae and use it as a framework to assess the evolution and diversification in mandible size and shape within the family. Opossum mandibles occupy a morphospace that is structured first by the difference in mandible shape between the genus *Caluromys* and all other species (with little allometry), and second by an allometric effect of size onto shape. This variation has a strong phylogenetic signal, and more closely related taxa form clusters in morphospace strongly influenced by phylogenetic proximity. Yet, specific events of morphological convergence and divergence are observed, as well as varying levels of morphological diversification in species-rich genera. Even though there are no clear differences between diets across genera, taxa with preferences for fruits or invertebrates form distinct groups. It remains unclear if this is due to functional demands or if it is merely a reflection of phylogeny,

Figure 6 Reconstruction of mandible ancestral size (left tree) and shape (right tree) onto the phylogeny obtained in this study, using squared-changed parsimony. Numbers on nodes and tips (left tree) represent reconstructed centroid sizes and average centroid size per species, respectively. Grids (right tree) represent either shapes of selected terminals (midline, along with a photo of a specimen of that species) or reconstructed shapes on selected nodes (indicated as A–J). An estimated reconstructed image is given in Supplementary Figure S2.

given that diet (as determined here) is also influenced by phylogeny. Nevertheless, overall omnivores and those with preferences for vertebrates overlap in morphospace, and these diets seem to be strongly influenced by size (all larger taxa fall within these two groups, as seen in Figure 5), being attainable by larger taxa only. Finally, we were able to detect events of mandible shape diversification concurrent with increase or decrease events along the phylogeny of Didelphidae, and our results suggest that the ancestral Didelphidae morphology was very similar to that of mouse opossums of the genus *Marmosa*, sub-genus *Micoureus*.

Phylogeny and diversification

The Didelphidae phylogeny provided here represents the most comprehensive time tree generated for the family. Our general results do not differ strongly from previous published phylogenetic analyses of Didelphidae, especially those by Voss and Jansa (2009), Amador and Giannini (2016), and Upham et al. (2019). The position of *Glironia* in the family is still controversial (Voss and Jansa 2021), and our phylogeny recovers *Glironia* as the sister group to Caluromyinae, although with only moderate support. The intergeneric relationships within the tribe Marmosini also remain controversial, as *Tlacuatzin* is often recovered as sister to the genus *Marmosa*, as in the phylogenetic hypotheses by Mitchell et al. (2014), Amador and Giannini (2016), or Upham et al. (2019), or as sister to a clade composed by *Monodelphis* + *Marmosa*, as recovered by Voss and Jansa (2021) and by our study.

Our results on intrageneric relationships also do not present noteworthy contrast with previous studies that sampled within Didelphidae genera. Some results that merit mention include (1) the strong support for *Monodelphis ronaldi* as sister to *M. handleyi*, corroborating the recent findings of Ruelas and Pacheco (2022), and supporting the recognition of *Monodelphis ronaldi* within the subgenus *Mygalodelphis*; (2) *T. pusillus* as a sister group to the clade that includes *T. citellus* and *T. pulchellus*, corroborating previous phylogenetic analyses (Teta et al. 2009; Palma et al. 2014); and (3) *M. meridae* as sister to the Phaea species-group (including *M. constantiae*, *Marmosa phaea*, and *M. demerarae*), in agreement with the phylogenetic results of Voss et al. (2020). The latter results indicate that the specimens identified as *M. meridae* are not most closely related nor nested within *M. demerarae* and therefore support its recognition as a separate terminal.

Our inferences on divergence times based on RelTime analysis do not present noteworthy contrast with published estimates based on relaxed-clock analyses using dense sampling within Didelphidae (e.g., Jansa et al. 2014; Beck and Taglioretti 2019), although our estimated dates for divergences are younger than estimates for crown-clade Didelphidae (median age 23 versus 24 Ma estimated by Beck and Taglioretti 2019, and 26 Ma estimated by Jansa et al. 2014 for the same node), and often older than estimates for intrageneric diversifications (e.g., median ages about 12 and 11 Ma for *Marmosops* and *Marmosa*, respectively, versus 9 and 10 Ma estimated by Beck and Taglioretti 2019, and

versus 10 and 10 Ma estimated by Jansa et al. 2014 for the same nodes). Differences between ours and previous estimates might be related to different datasets used, distinct calibration points, and distinct methods of inference used in the different analyses.

Mandible shape and size

Didelphid marsupials are generally considered to be a morphologically conservative group with generalist feeding habits. Although didelphids are known for these characteristics, our results indicate that their mandibles showed considerable variation in shape (Figure 3). Despite the large overlap between most lineages, Caluromyinae and the Didelphini occupy a distinct region in morphospace. Didelphidae body sizes range from about 10 g in adult *Hyladelphys* and *Gracilinanus* up to 5 kg in *D. virginiana* (Amador and Giannini 2016; Voss and Jansa 2021). Similarly, calculated mandible sizes ranged from 27.43 mm in a specimen of *Monodelphis kunsi* to 155.81 mm in a specimen of *D. virginiana*. Yet, our results point out that despite this great disparity in mandible sizes (due to the increase in body size in Caluromyinae, Didelphini, and Metachirini), and previous analyses indicating that size is an important factor in the shape variation of some structures (Astúa 2009; Chemisquy et al. 2021), the role of allometry on the morphological diversity of didelphid mandibles was lower than expected, at least as the major driver of shape change. Morphospace (Figures 3 and 4) is driven first by the shape variation between Caluromyinae and all remaining Didelphidae (ca. 40% of all variation in either approach, with a low correlation with size variation), and only the second major axis of variation is strongly correlated with size, thus indicating an axis of allometric variation. This interestingly contrasts with the variation found in the Didelphidae scapula, where the first component of shape variation was clearly allometric (Astúa 2009). It also contrasts with the variation found in the Didelphidae cranium, where the first component of shape variation for all three cranial views was also allometric (Chemisquy et al. 2021), including the lateral view, which could be expected to co-vary closely with the mandible as captured here. The distinction between the mandible of Caluromyinae and all other Didelphidae is not allometric, especially because the former, located at the negative scores of the main axis of shape variation, are of intermediate size, while the specimens located at the positive scores of that axis include both the largest and smallest species (including several overlapping in size with Caluromyinae). This pattern is unexpected because size has been constantly reported as the main driver of variation in Didelphidae (Shirai and Marroig 2010; Sebastião and Marroig 2013; Flores et al. 2018) and even across marsupials (Giannini et al. 2021; Flores et al. 2022). Yet it is so strong that it drives the ordination of mandible morphospace even when other orders are incorporated in the comparison, including the highly morphologically divergent mandibles of Paucituberculata, as Brum et al. (2022) recently found.

Within Caluromyinae, the *Caluromys* mandible shape is the most distinctive and clearly divergent from other Didelphidae (Figures 3 and 4). In fact, *Caluromys* mandibles have unique features within the family, such as the well-developed coronoid process and an angular process that is not medially inflected, unlike all other Didelphidae (Sánchez-Villagra and Smith 1997). This, alone, is not sufficient to account for all the differences in the *Caluromys* mandible, as it includes a very short and broad horizontal ramus and a caudally inflected coronoid process. Strength and shortening of the horizontal ramus could be related to an increase in bite force, through the reduction of the moment arm of the applied force, but no actual estimates of bite force in Didelphidae exist except for *Didelphis* (Thomason et al. 1990; Thomason 1991). Thus, such inference still needs additional empirical or modeled data for a proper evaluation. Prevosti et al. (2012) included a few *Caluromys* specimens in their comparison between placental and marsupial carnivorous mandibles. While they do not explicitly identify those specimens in their PCA plots, they are labeled as Didelphidae "herbivore" and probably are the data points toward the positive scores of their PC1, overlapping with some taxa labeled as hypercarnivores or omnivores, and sharing with those a broad horizontal ramus. In turn, the inflection of the coronoid process had been noted by Astúa de Moraes et al. (2000) and had been hypothesized to adjust for gape in a more ventrally arched cranium, also noticeable yet to a lesser extent in the larger sample analyzed by Chemisquy et al. (2021).

While the main axes of shape variation are driven by the divergence between Caluromyinae and all other taxa firstly, and by size secondly, a close inspection of mandible phylomorphospace reveals several interesting events of divergence (within groups) or convergences (between groups), or even varying levels of morphospace occupation unrelated to species richness (at the genus level). Caluromyinae does not constitute a uniform group, as *Caluromys* and *Caluromysiops* are highly divergent, with the latter closer to the morphospace of the Didelphini. In fact, the divergence between these two genera spans a distance in morphospace that is greater than the largest span in Didelphini morphospace, and comparable to the Marmosini morphospace, and the two genera are more distanced than whole subfamilies or tribes that diverged much earlier (e.g., Hyladelphinae, Marmosini, and Didelphini) are. *Glironia venusta* exhibits unusual morphological traits not seen or rarely seen in other didelphids (Voss and Jansa 2021). The position of *G. venusta* in the Didelphidae phylogeny is uncertain, and it may be a sister group to all other didelphids, the sister group to Hyladelphinae + Didelphinae, or the sister group to Caluromyinae (see Figure 34 in Voss and Jansa 2009), as observed in our reconstructed phylogeny (Voss and Jansa 2009; Mitchell et al. 2014). However, *Glironia* mandible size and shape are very different from *Caluromys* and *Caluromysiops*. *Glironia* has a small and slender mandible and a well-developed angular process, thus more similar to the Didelphidae ancestor than to the Caluromyinae. This retention of the generalized ancestral morphology in *Glironia* explains its position in morphospace (within the morphospaces of Thylamyini and Marmosini), and supports the hypothesis that the unique mandible morphology of Caluromyinae evolved after they diverged. Therefore, any inference on *Glironia* ecology based on Caluromyinae is speculative and unsupported, given their marked morphological divergence (Figure 4). Another noteworthy divergence is observed in the small *Hyladelphys*, one of the smallest Didelphidae, which has a combination of the caudally-inflected coronoid process with the slender horizontal ramus of most small opossums (Figure 6). Hyladelphinae is another poorly known group whereas inference of the relation between mandible morphology and ecology is still precluded. Such as *Glironia* and *Caluromysiops*, this group awaits much-needed ecological

data for an adequate appraisal of form-function relationships (Astúa 2015; Astúa and Guilhon 2022).

Didelphini groups the current didelphid species with the largest body sizes, ranging from approximately 300 g to approximately 5 kg in adult specimens (Voss and Jansa 2021). Although *Metachirus* is phylogenetically related to Didelphini, it is positioned within the Marmosini morphospace, overlapping only partially with Didelphini (Figure 3), see also its divergence in Brum et al. (2022). Despite the increase in body size, the *Metachirus* mandible has not changed as much in its shape, retaining a more plesiomorphic shape. As size increase is more pronounced after the divergence of Metachirini from Didelphini (Figure 6), the retention of the more slender shape in *Metachirus* (as compared to the most robust, allometry-related shapes of Didelphini) may correlate with its preference for invertebrates despite its size, when compared to *Didelphis* or *Philander*, even with the same resources available (Freitas et al. 1997; Santori et al. 1997).

Didelphidae diversity is unequally distributed across genera, with several monotypic (*Hyladelphys*, *Glironia*, and *Caluromysiops*) genera, while others are highly speciose, such as *Monodelphis*, *Marmosa*, or *Marmosops* (Astúa et al. 2022; Voss 2022). While it is natural to expect that speciose genera spread throughout a wider portion of morphospace (because species diverge in size or shape from the genus ancestor in possibly more directions), speciose genera do not occupy comparable portions of morphospace: some, such as *Monodelphis*, have its species spread farther apart from each other than other genera, such as *Marmosops* or *Marmosa*. The factors underlying these differences remain unclear and merit further investigation. It is well known that some *Monodelphis* species exhibit striking levels of sexual dimorphism, in shape and size (Astúa 2010; Chemisquy 2015). This could be influencing the position of these species in morphospace (even though we use the centroid for the species to plot species positions in morphospaces). It does not seem the case, as, for example, one of the most dimorphic species, *Monodelphis dimidiata*, is positioned closer to the overall centroid of the genus morphospace (data not shown). The genus *Monodelphis* constitutes a remarkable radiation within Didelphidae, with marked phenotypic and ecological diversification (Pavan 2022). A similar appraisal of morphological and ecological variation within the genera *Marmosa* or *Marmosops* is still unavailable, and, likely, a comparative approach of diversification patterns and rates across these three genera may shed some light on the differences in morphospace occupation.

Mandibular morphology and diet

Our current knowledge of Didelphidae diet data comes mostly from the examination of feces or stomach contents, fortuitous observation of free-ranging animals in their native habitats, and experiments with captive specimens, complemented by data from stable isotope analyses from very few taxa (Lessa et al. 2022). Only a few species of didelphids have a well-known diet (i.e., based on several studies at different locations with adequately quantified items or categories), and no didelphid feeds only on one food category (Astúa 2015; Lessa et al. 2022). The definition of dietary categories has always been a controversial issue, and except for species with a very restricted diet (which do not occur in Didelphidae), there is usually an overlap of categories, and as currently understood, opossum dietary habits form a continuum of different levels of food preferences (Astúa de Moraes et al. 2003; Voss and Jansa 2021). Pineda-Munoz and Alroy (2014) created a diet classification scheme for mammals based on the most frequently consumed food resource. They suggested classifying a species into a specialist if a single food resource is part of 50% or more of the diet. However, most species of didelphids do not have their diet described by studies specifically focused on this purpose (Lessa et al. 2022). In addition, the vast majority of diet studies on opossums, based on fecal samples, use frequency of occurrence data, which do not allow a proper assessment of the relative importance of items or putative categories in each species' diet. The categories we used here to classify the Didelphidae diet are intentionally coarse to reflect this uncertainty, because, in general, a mixed diet of invertebrates (mainly insects) and fruits characterize most didelphids, with many, even smaller species, known to include some vertebrate as well (Voss and Jansa 2021; Lessa et al. 2022). In addition to that uncertainty, diets also vary according to the availability and seasonality of food resources, as well as geographically (Lessa et al. 2022).

Those caveats should thus be reminded when interpreting relations between Didelphidae morphology and diet, both at higher (e.g., Chemisquy et al. 2021; Brum et al. 2022; Bubadué et al. 2022) or lower taxonomic levels (e.g., Cáceres et al. 2016; Magnus et al. 2017). At first inspection, even with our coarse categories, it would seem that the Didelphidae morphospace is structured by "diet," with a portion occupied by those omnivores with fruit preference, a portion occupied by those with invertebrate preferences, and another occupied by both those with vertebrate preferences and those recognized as straight omnivores (Figure 5). Yet this structure mixes ecological, phylogenetic, and allometric factors. The omnivore with a preference for fruits is mostly the morphospace portion occupied by *Caluromys*, but it is unclear if (1) they can truly be considered with a preference for fruits, as they may easily shift to a more insectivore diet and even consume vertebrates (Lessa et al. 2022), (2) all species really share the same preferences, as most of what is known from *C. philander* and to a lesser extent, *C. lanatus* (Cáceres and Carmignotto 2006; Astúa 2015), and (3) there is a relation between the unique mandibular morphology of *Caluromys* and a more "frugivorous" diet. Mandible shape could be divergent for other evolutionary reasons (e.g., correlated evolution with any cranial feature not seen here), and its correlation with its diet be spurious. The main feature distinguishing *Caluromys* is located at the angular process. The medial inflection of the angular process, typical of most marsupials, is absent in *Caluromys* (Sánchez-Villagra and Smith 1997) resulting in a bulkier aspect of the posterior end of the horizontal ramus below the masseteric fossa (when seen from a lateral view) compared to all other Didelphidae, which have well-defined and inflected angular processes. The loss of this inflection has occurred independently in different marsupial lineages and can hardly be related to diet, having also occurred in the ant-eating numbats (*Myrmecobius*), the nectarivorous honey possums (*Tarsipes*), the folivorous koalas (*Phascolarctos*), and the insectivorous striped possums (*Dactylopsila*) (Sánchez-Villagra and Smith 1997). Thus, until we understand properly not only the ecology but also the mechanics and muscular anatomy of opossums (Astúa and Guilhon 2022), no further functional inferences can be made on this unique morphology of woolly opossums.

The morphospace occupied by omnivores and those with vertebrate preferences is actually the morphospace of Didelphini, as it is within this tribe that these two categories were established. This similarity between Didelphini mandibles had already been reported by Astúa de Moraes et al. (2000). Within Didelphini, the most striking cranial feature usually associated with a more efficient bite force (and thus interpreted as a more carnivore-prone diet) is the shortening of the rostrum in *Lutreolina* and other extinct taxa (Beck and Taglioretti 2019; Astúa and Guilhon 2022). This feature was noted by Astúa de Moraes et al. (2000) and seems to appear in the analyses of Chemisquy et al. (2021), although their graphics do not allow to recognize individual genera. Nevertheless, this difference is not clearly reflected in mandibular morphology, as morphospace occupation by *Lutreolina* is comparable to that of other Didelphini (Figure 4). As such, it seems that at least as far as mandible morphology is concerned, the overall increase in size (and consequent allometry-driven increase in robustness) allowed for a diversification of the Didelphidae diet, both because of the obvious capacity to predate larger taxa, but also due to possible allometric increase in bite force. Brum et al. (2022) showed that the Didelphini have faster evolutionary rates for size, and related this increase in size to access to more energetically valuable items. It will thus be very interesting to gain a better understanding of the diet and functional requirements of *Caluromysiops*, for example, to understand its divergence from the Caluromyinae morphospace toward the Didelphini morphospace (Figures 4 and 5), as it could represent a convergence toward this stronger and more versatile morphology.

Didelphid mandible evolution

The reconstruction of ancestral mandible size and shape indicates that the living didelphids evolved from an ancestor with a mandible of the size of that of *Marmosa* species (mainly from the subgenus *Micoureus*) and *Gironia* and with a shape similar to that of *Marmosa* and *Thylamys* species (Figure 6). These findings are similar to those found by Astúa (2009) for the scapula of Didelphidae whereas ancestral size was found to correspond to that of *Gironia* and *Marmosa* (*Micoureus*) and shapes closely resemble those of *Marmosa* (*Micoureus*) and *Gracilinanus*. As per our results, the mandible shape in *Gracilinanus* is also similar to that of the ancestral Didelphidae.

The only other comprehensive study to look into the evolution of size in Didelphidae was that of Amador and Giannini (2016), which used a sample of ca. 80% of all recognized taxa at the time, but they used body mass as a measure of size. Their findings point to a smaller (lighter) Didelphidae ancestor than what we have found here, but the main events are similar to those we report, with marked increases in size found at the roots of the Didelphini + Metachirini and the Caluromyinae clades, and reductions in Thylamyini and Marmosini. Their results also detected that the magnitudes in events of increase are much more pronounced than those of size decrease events. Even though they noted that, given the small body mass found in their reconstruction, increases were more likely to occur than decreases (Amador and Giannini 2016), and Brum et al. (2022) also found higher evolutionary rates for size in clades with larger species, such as Didelphini and Caluromyinae, supporting the distinctiveness of these events.

One important feature we were able to retrieve from our analyses is the timing of some of these events. The two main change events in size and shape in the Didelphidae mandible (Figure 6) had their onset at the root of the Caluromyinae and Didelphini + Metachirini clades and resulted in the two most divergent groups in the family (Figures 3 and 4). An inspection of the timing of these events (Figure 2) shows that both occurred independently within a timeframe ranging from 9 to 13 Mya, while the onset of reductions (in Marmosini, Thylamyini, or Hyladelphinae) is older. Because the increase in size is related to major shape changes (due to allometry) and these two clades represent the most divergent mandibular morphologies, it is interesting that they seem to have occurred independently within a relatively narrow period. What could be the biotic or abiotic events related to this increase in size, and thus in shape and diet variety attainable remains to be better investigated, but this is the first time that this coincidence in timing is reported.

The overall ancestral mandible for Didelphidae was that of an intermediate to small opossum, with a generalized shape. Because Didelphidae diets are mostly overlapping at least on food categories used and there is yet no adequate quantitative way to compare the different (and still scarce) diet studies existing for some taxa, this morphology could only tentatively be related to any diet. As far as we know, however, most small didelphids included important amounts of invertebrates in their diets, whether from actual preference or simply because it could be the most abundant food source available in their size range (Lessa et al. 2022). This morphology would thus be compatible with a diet with important amounts of invertebrates at the origin of the Didelphidae radiation, as found by Amador and Giannini (2020). This unspecialized morphology would thus be retained in most small opossums and would have diverged in those lineages that increased in size, resulting in different shapes due to allometry and allowing other food resources to be incorporated more easily into their diets, even if no strict specialization is attained.

Chemisquy et al. (2021) noted that the morphospace of cranial shapes was organized more according to size and phylogenetic relationships than to diet, or habitat use, suggesting that didelphids are responding to size changes to selection pressures imposed by ecological characteristics. Brum et al. (2022) concluded that mandible size variation was partially explained by diet. Despite the previously stated possible limitations of the level of specificity in their dietary classification, we agree that size represents an important axis for morphological diversification in opossums, and size variation can lead to niche differentiation. It remains however unclear how the cranium and mandible have coevolved along the Didelphidae radiation. Therefore, both an adequate dietary scheme and an integrated analysis of cranial and mandibular shape evolution are strongly needed to better understand the morphological and ecological diversification of opossums.

Author Contributions

FCS-N, DA: Conceptualization, choosing methods, conducting the research, data interpretation, and writing of the geometric morphometric portion of the manuscript. FCS-N, SEP: Choosing methods, conducting the research, data interpretation, and writing the phylogenetic portion of the manuscript. DA, SP: Collected mandible images of the specimens. DA: Digitized landmarks. FCS-N: Digitized semi-landmarks. FCS-N, DA, SEP: Data analysis, commenting, and editing drafts of the manuscript.

Data Availability

Files with the phylogeny and bootstrap values, and with the dated phylogeny are provided as Supplementary data. Other data are available from the authors upon reasonable request.

Conflict of Interest Statement

All authors declare no conflicts of interest.

Supplementary Material

Supplementary material can be found at https://academic.oup.com/cz.

References

Adams DC, 2014. A method for assessing phylogenetic least squares models for shape and other high-dimensional multivariate data. *Evolution* **68**:2675–2688.

Adams DC, Collyer ML, Kaliontzopoulou A, Baken EK, 2022. *Geomorph: Software for Geometric Morphometric Analyses*. R package version 4.0.4. https://cran.r-project.org/package=geomorph.

Álvarez A, Perez SI, Verzi DH, 2011. Ecological and phylogenetic influence on mandible shape variation of South American caviomorph rodents (Rodentia: Hystricomorpha). *Biol J Linn Soc* **102**:828–837.

Amador LI, Giannini NP, 2016. Phylogeny and evolution of body mass in didelphid marsupials (Marsupialia: Didelphimorphia: Didelphidae). *Org Divers Evol* **16**:641–657.

Amador LI, Giannini NP, 2020. Evolution of diet in extant marsupials: Emergent patterns from a broad phylogenetic perspective. *Mammal Rev* **51**:178–192.

Astúa D, 2009. Evolution of scapula size and shape in didelphid marsupials (Didelphimorphia: Didelphidae). *Evolution* **63**:2438–2456.

Astúa D, 2010. Cranial sexual dimorphism in New World marsupials and a test of Rensch's rule in Didelphidae. *J Mammal* **91**:1011–1024.

Astúa D, 2015. Family Didelphidae (Opossums). In: Wilson DE, Mittermeier RA, editors. *Handbook of the Mammals of the World. Vol. 5: Monotremes and Marsupials*. Barcelona: Lynx Edicions/Conservation International/ IUCN, 70–186.

Astúa D, Cherem JJ, Teta P, 2022. Taxonomic checklist of living American marsupials. In: Cáceres N, Dickman CR, editors. *American and Australasian Marsupials*. Cham: Springer, doi:10.1007/978-3-030-88800-8_31-1.

Astúa D, Guilhon GN, 2022. Morphology, form and function in didelphid marsupials. In: Cáceres N, Dickman CR, editors. *American and Australasian Marsupials*. Cham: Springer, doi:10.1007/978-3-030-88800-8_8-1.

Astúa D, Leiner NO, 2008. Tooth eruption sequence and replacement pattern in woolly opossums, genus *Caluromys* (Didelphimorphia: Didelphidae). *J Mammal* **89**:244–251.

Astúa de Moraes D, Hingst-Zaher E, Marcus LF, Cerqueira R, 2000. A geometric morphometric analysis of cranial and mandibular shape variation of didelphid marsupials. *Hystrix (n.s)* **11**:115–130.

Astúa de Moraes D, Santori RT, Finotti R, Cerqueira R, 2003. Nutritional and fibre contents of laboratory-established diets of neotropical opossums (Didelphidae). In: Jones ME, Dickman CR, Archer M, editors. *Predators with Pouches: The Biology of Carnivorous Marsupials*. Collingwood: CSIRO Publishing, 221–237.

Atramentowicz M, 1988. La frugivorie opportuniste de trois marsupiaux didelphidés de Guyane. *Rev Ecol (Terre et Vie)* **43**:47–57.

Baken EK, Collyer ML, Kaliontzopoulou A, Adams DC, 2021. geomorph v4.0 and gmShiny: enhanced analytics and a new graphical interface for a comprehensive morphometric experience. *Methods Ecol Evol* **12**:2355–2363.

Beck RMD, Taglioretti ML, 2019. A nearly complete juvenile skull of the marsupial *Sparassocynus derivatus* from the Pliocene of Argentina, the affinities of "Sparassocynids," and the diversification of opossums (Marsupialia; Didelphimorphia; Didelphidae). *J Mamm Evol* **27**:385–417.

Bennett CV, Goswami A, 2013. Statistical support for the hypothesis of developmental constraint in marsupial skull evolution. *BMC Biol* **11**:52.

Bookstein FL, 1997. Landmark methods for forms without landmarks: morphometrics of group differences in outline shape. *Med Image Anal* **1**:225–243.

Bookstein FL, 2018. *A Course in Morphometrics for Biologists: Geometry and Statistics for Studies of Organismal Form*. Cambridge: Cambridge University Press.

Bookstein FL, 2021. Centric allometry: studying growth using landmark data. *Evol Biol* **48**:129–159.

Brum MN, Cáceres NC, Bubadué JM, 2022. Evolutionary rates, disparity, and ecomorphology of the mandible in American marsupials. *J Mamm Evol* **30**:33–46.

Bubadué J, Cáceres N, Brum M, Meloro C, 2022. Skull morphological evolution in faunivorous marsupials. In: Cáceres NC, Dickman CR, editors. *American and Australasian Marsupials*. Cham: Springer, doi:10.1007/978-3-030-88800-8_7-1.

Cáceres NC, Carmignotto AP, 2006. *Caluromys lanatus*. *Mamm Species* **803**:1–6.

Cáceres NC, de Moraes Weber M, Melo GL, Meloro C, Sponchiado J et al., 2016. Which factors determine spatial segregation in the South American opossums (*Didelphis aurita* and *D. albiventris*)? An ecological niche modelling and geometric morphometrics approach. *PLoS ONE* **11**:e0157723.

Chemisquy MA, 2015. Peramorphic males and extreme sexual dimorphism in *Monodelphis dimidiata* (Didelphidae). *Zoomorphology* **184**:587–599.

Chemisquy MA, Prevosti FJ, Martin G, Flores D, 2015. Evolution of molar shape in didelphid marsupials (Marsupialia: Didelphidae): analysis

of the influence of ecological factors and phylogenetic legacy. *Zool J Linn Soc* **173**:217–235.

Chemisquy MA, Tarquini SD, Romano Muñoz CO, Prevosti FJ, 2021. Form, function and evolution of the skull of didelphid marsupials (Didelphimorphia: Didelphidae). *J Mamm Evol* **28**:23–33.

Christiansen P, 2008. Evolution of skull and mandible shape in cats (Carnivora: Felidae). *PLoS One* **3**:e2807.

Clark CT, Smith KK, 1993. Cranial osteogenesis in *Monodelphis domestica* (Didelphidae) and *Macropus eugenii* (Macropodidae). *J Morphol* **215**:119–149.

Edgar RC, 2004. MUSCLE: multiple sequence alignment with high accuracy and high throughput. *Nucleic Acids Res* **32**:1792–1797.

Falconer DS, Mackay TFC, 2009. *Introduction to Quantitative Genetics*. 4th edn. Essex: Longman.

Flores DA, Abdala F, Giannini NP, 2022. Postweaning skull growth in living American and Australasian marsupials: allometry and evolution. In: Cáceres N, Dickman CR, editors. *American and Australasian Marsupials*. Cham: Springer, doi:10.1007/978-3-030-88800-8_6-1.

Flores DA, Giannini N, Abdala F, 2018. Evolution of post-weaning skull ontogeny in New World opossums (Didelphidae). *Org Divers Evol* **18**:367–382.

Freitas SR, Astúa de Moraes D, Santori RT, Cerqueira R, 1997. Habitat preference and food use by *Metachirus nudicaudatus* and *Didelphis aurita* (Didelphimorphia, Didelphidae) in a restinga forest at Rio de Janeiro. *Rev Bras Biol* **57**:93–98.

Gemmell RT, Veitch C, Nelson J, 2002. Birth in marsupials. *Comp Biochem Physiol B Biochem Mol Biol* **131**:621–630.

Giannini NP, Morales MM, Wilson LAB, Velazco PM, Abdala F et al., 2021. The cranial morphospace of extant marsupials. *J Mamm Evol* **28**:1145–1160.

Goin FJ, Woodburne MO, Zimicz AN, Martin GM, Chornogubsky L, 2016. *A Brief History of South American Metatherians: Evolutionary Contexts and Intercontinental Dispersals*. Dordrecht: Springer.

Giarla TC, Voss RS, Jansa SA, 2010. Species limits and phylogenetic relationships in the didelphid marsupial genus *Thylamys* based on mitochondrial DNA sequences and morphology. *Bull Am Mus Nat Hist*. **346**: 3-67.

Goswami A, Polly PD, Mock OB, Sanchez-Villagra MR, 2012. Shape, variance and integration during craniogenesis: contrasting marsupial and placental mammals. *J Evol Biol* **25**:862–872.

Hammer O, Harpee D, Ryan P, 2001. Past: Paleontological statistics software package for education and data analysis. *Palaeontol Electronica* **4**:1–9.

Jansa SA, Barker FK, Voss RS, 2014. The early diversification history of didelphid marsupials: A window into South America's "Splendid Isolation." *Evolution* **68**:684–695.

Klingenberg CP, 2011. MorphoJ: An integrated software package for geometric morphometrics. *Mol Ecol Resour* **11**:353–357.

Klingenberg CP, 2013. Visualizations in geometric morphometrics: How to read and how to make graphs showing shape changes. *Hystrix* **24**:15–24. doi:10.4404/hystrix-24.1-7691.

Klingenberg CP, 2016. Size, shape, and form: concepts of allometry in geometric morphometrics. *Dev Genes Evol* **226**:113–137.

Klingenberg CP, Gidaszewski NA, 2010. Testing and quantifying phylogenetic signals and homoplasy in morphometric data. *Syst Biol* **59**:245–261.

Lanfear R, Frandsen PB, Wright AM, Senfeld T, Calcott B, 2017. PartitionFinder 2: new methods for selecting partitioned models of evolution for molecular and morphological phylogenetic analyses. *Mol Biol Evol* **34**:772–773.

Lessa LG, Carvalho RF, Astúa D, 2022. Food habits of American marsupials. In: Cáceres N, Dickman CR, editors. *American and Australasian Marsupials*. Cham: Springer, doi:10.1007/978-3-030-88800-8_22-2.

Letunic I, Bork P, 2021. Interactive Tree of Life (iTOL) v5: an online tool for phylogenetic tree display and annotation. *Nucleic Acids Res* **49**:W293–W296.

Maddison WP, Maddison DR, 2021. Mesquite: a modular system for evolutionary analysis. Version 3.70. http://www.mesquiteproject.org

Magnus LZ, Cáceres N, 2017. Phylogeny explains better than ecology or body size the variation of the first lower molar in didelphid marsupials. *Mammalia* **81**:119–133.

Magnus LZ, Machado RF, Cáceres N, 2017. Comparative ecogeographical variation in skull size and shape of two species of woolly opossums (genus *Caluromys*). *Zool Anz* **267**:139–150.

Martins EP, Hansen TF, 1997. Phylogenies and the comparative method: A general approach to incorporating phylogenetic information into the analysis of interspecific data. *Am Nat* **149**:646–667.

Meloro C, Caceres NC, Carotenuto F, Sponchiado J, Melo GL et al., 2015. Chewing on the trees: Constraints and adaptation in the evolution of the primate mandible. *Evolution* **69**:1690–1700.

Miller M, Pfeiffer W, Schwartz T, 2010. Creating the CIPRES science gateway for inference of large phylogenetic trees. *2010 Gateway Computing Environments Workshop (GCE)*. IEEE: New Orleans, LA, USA, 1–8. doi: 10.1109/GCE.2010.5676129

Miranda CL, Nunes MS, Fabrício Machado A, Farias IP, Menezes FH et al., 2023. A new species of jupati, genus *Metachirus* Burmeister 1854 (Didelphimorphia, Didelphidae) for the Brazilian Amazon. *Mammalia* **87**:172–189.

Mitchell KJ, Pratt RC, Watson LN, Gibb GC, Llamas B et al., 2014. Molecular phylogeny, biogeography, and habitat preference evolution of marsupials. *Mol Biol Evol* **31**:2322–2330.

Palma RE, Boric-Bargetto D, Jayat JP, Flores DA, Zeballos H et al., 2014. Molecular phylogenetics of mouse opossums: new findings on the phylogeny of *Thylamys* (Didelphimorphia, Didelphidae). *Zoologica Scripta* **43**(3):217–234.

Pavan SE, 2022. Short-tailed opossums genus *Monodelphis*: Patterns of phenotypic evolution and diversification. In: Cáceres N, Dickman CR, editors. *American and Australasian Marsupials*. Cham: Springer, https://doi.org/10.1007/978-3-030-88800-8_10-1

Pineda-Munoz S, Alroy J, 2014. Dietary characterization of terrestrial mammals. *Proc Biol Sci* **281**:20141173.

Prevosti FJ, Turazzini GF, Ercoli MD, Hingst-Zaher E, 2012. Mandible shape in marsupial and placental carnivorous mammals: A morphological comparative study using geometric morphometrics. *Zool J Linn Soc* **164**:836–855.

R Core Team. 2021. *R: A Language and Environment for Statistical Computing*. Vienna: R Foundation for Statistical Computing. URL https://www.R-project.org/

Raia P, Carotenuto F, Meloro C, Piras P, Pushkina D, 2010. The shape of contention: Adaptation, history, and contingency in ungulate mandibles. *Evolution* **64**:1489–1503.

Rohlf FJ, 2015. The tps series of software. *Hystrix* **26**:9–12.

Rohlf FJ, Slice D, 1990. Extensions of the Procrustes method for the optimal superimposition of landmarks. *Syst Zool* **39**:40–59.

Ruelas D, Pacheco V, 2022. New morphological data and phylogenetic position of the rare short-tailed opossum *Monodelphis ronaldi* (Didelphimorphia: Didelphidae) with new records. *Mamm Biol* **102**:189–204.

Sánchez-Villagra MR, Smith KK, 1997. Diversity and evolution of the marsupial mandibular angular process. *J Mamm Evol* **4**:119–144.

Santori RT, Astúa de Moraes D, Grelle CEV, Cerqueira R, 1997. Natural diet at a Restinga forest and laboratory food preferences of the opossum *Philander frenata* in Brazil. *Stud Neotrop Fauna Environ* **32**:12–16.

Santori RT, Lessa LG, Astúa D, 2012. Alimentação, nutrição e adaptações alimentares de marsupiais brasileiros. In: Cáceres NC, editor. *Os marsupiais do Brasil: biologia, ecologia e conservação*. Campo Grande, MS: Editora UFMS, 384–406.

Schwarz G, 1978. Estimating the dimension of a model. *Ann Stat* **6**:461–464.

Sebastião H, Marroig G, 2013. Size and shape in cranial evolution of 2 marsupial genera: *Didelphis* and *Philander* (Didelphimorphia, Didelphidae). *J Mammal* **94**(6):1424–1437.

Shirai LT, Marroig G, 2010. Skull modularity in Neotropical marsupials and monkeys: Size variation and evolutionary constraint and flexibility. *J Exp Zoolog B Mol Dev Evol* **314B**:663–683.

Sidlauskas B, 2008. Continuous and arrested morphological diversification in sister clades of characiform fishes: A phylomorphospace approach. *Evolution* **62**:3135–3156.

Silva LGDL, Ferreira DC, Rossi RV, 2019. Species diversity of *Marmosa* subgenus *Micoureus* (Didelphimorphia, Didelphidae) and taxonomic evaluation of the white-bellied woolly mouse opossum *Marmosa constantiae*. *Zool J Linn Soc* **187**:240–277.

Sukumaran J, Holder MT, 2010. DendroPy: a Python library for phylogenetic computing. *Bioinformatics* **26**:1569–1571.

Tamura K, Stecher G, Kumar S, 2021. MEGA11: Molecular Evolutionary Genetics Analysis. Version 11. *Mol Biol Evol* **38**:3022–3027.

Tamura K, Tao Q, Kumar S, 2018. Theoretical foundation of the RelTime method for estimating divergence times from variable evolutionary rates. *Mol Biol Evol* **35**:1770–1782.

Teta P, Abba AM, Cassini GH, Flores DA, Galliari CA et al., 2018. Lista revisada de los mamÍferos de Argentina. *Mastozool Neotrop* **25**:163–198.

Teta P, D'Elía G, Flores D, de la Sancha N, 2009. Diversity and distribution of the mouse opossums of the genus *Thylamys* (Didelphimorphia, Didelphidae) in northeastern and central Argentina. *Gayana* **73**:180–199.

Thomason JJ, 1991. Cranial strength in relation to estimated biting forces in some mammals. *Can J Zool* **69**:2326–2333.

Thomason JJ, Russell AP, Morgeli M, 1990. Forces of biting, body size, and masticatory muscle tension in the opossum *Didelphis virginiana*. *Can J Zool* **68**:318–324.

Tribe CJ, 1990. Dental age classes in *Marmosa incana* and other didelphoids. *J Mammal* **71**:566–569.

Tyndale-Biscoe CH, Mackenzie RB, 1976. Reproduction in *Didelphis marsupialis* and *D. albiventris* in Colombia. *J Mammal* **57**:249–265.

Upham NS, Esselstyn JA, Jetz W, 2019. Inferring the mammal tree: species-level sets of phylogenies for questions in ecology, evolution, and conservation. *PLoS Biol* **17**:e3000494.

Vieira EM, Astúa de Moraes D, 2003. Carnivory and insectivory in neotropical marsupials. In: Jones ME, Dickman CR, Archer M, editors. *Predators with Pouches: The Biology of Carnivorous Marsupials*. Collingwood: CSIRO Publishing, 271–284.

Voss RS, 2022. An annotated checklist of recent opossums (Mammalia: Didelphidae). *Bull Am Mus Nat Hist* **455**:1–74.

Voss RS, Giarla TC, Díaz-Nieto JF, Jansa SA, 2020. A revision of the didelphid marsupial genus *Marmosa* part 2. Species of the Rapposa group (Subgenus *Micoureus*). *Bull Am Mus Nat Hist* **439**:1–60.

Voss RS, Jansa SA, 2009. Phylogenetic relationships and classification of Didelphid marsupials, an extant radiation of New World Metatherian mammals. *Bull Am Mus Nat Hist* **322**:1–177.

Voss RS, Jansa SA, 2021. *Opossums: An Adaptive Radiation of New World Marsupials*. Baltimore: Johns Hopkins University Press.

Zwickl DJ, 2006. *Genetic Algorithm Approaches for the Phylogenetic Analysis of Large Biological Sequence Datasets under the Maximum Likelihood Criterion*. PhD dissertation. School of Biological Sciences, The University of Texas at Austin, Austin, Texas.